

Theory of hyperfine interactions in potassium and Sc^{2+} ion: Trends in systems isoelectronic with potassium

Alfred Owusu, Xing Yuan, S. N. Panigrahy, R. W. Dougherty, and T. P. Das
Department of Physics, State University of New York at Albany, Albany, New York 12222

J. Andriessen

Technische Natuurkunde, Technische Universiteit Delft, 2628 CJ Delft, The Netherlands

(Received 13 May 1996)

A first-principles relativistic many-body investigation of magnetic hyperfine fields has been carried out for the ground states $4^2S_{1/2}$ of the alkali atom K and doubly charged ion Sc^{2+} completing the investigation over the three members of the isoelectronic series K, Ca^+ , and Sc^{2+} with a single valence electron in the $4s$ state, since Ca^+ had been investigated by us previously. This allows one to study both the nature of agreement with experiment over this series as the charge increases and the trends in the contributions from the major mechanisms responsible for the hyperfine fields in these systems. The calculated magnetic hyperfine fields in tesla for K, Ca^+ , and Sc^{2+} are 56.81, 135.90, and 239.29, respectively. These agree very well with the measured values of 58.02 T for K and 140.30 T for Ca^+ . No experimental data are available for the Sc^{2+} system. The exchange core polarization (ECP) and correlation contributions, as fractions of the valence contribution, are found to decrease rapidly as one goes to systems with higher ionic charges, the decrease being more drastic for correlation effects. The trend of the ratios of ECP and correlation contributions to the valence contribution for both K and Sc^{2+} were compared with those calculated for the neighboring alkali-metal systems, sodium and rubidium. The physical explanations for the results and the observed trends in the contributions from the different mechanisms are discussed. [S1050-2947(97)04603-9]

PACS number(s): 31.10.+z, 31.25.Eb, 31.30.Gs, 31.30.Jv

I. INTRODUCTION

The relativistic linked-cluster many-body perturbation theory (RLCMBPT) [1] procedure has been extensively and successfully used to study hyperfine properties of atomic systems [2]. The first-principles investigation of the contributions to the hyperfine interactions in alkali-metal atoms [3] by RLCMBPT was central to the understanding of the theory. This is due to the fact that these systems are relatively simple and the contributions of the different physical effects, such as valence, exchange core polarization, and many-body effects, could be studied in considerable detail and accurately. These studies have also helped provide an understanding of the trends followed by the contributions to the hyperfine fields at the nuclei from different physical mechanisms over the alkali-metal atom series. Corresponding trends in other related systems [4], namely, the alkaline-earth series, the noble-metal atoms, and their partner isoelectronic singly charged Zn^+ , Cd^+ , and Ag^+ ions and in a series of lithiumlike systems [5], have also been investigated using this procedure. The trends of exchange core polarization (ECP) and correlation effects among and within these series studied provide a better physical understanding of the hyperfine interaction. The present work is concerned with the hyperfine interaction in K, Ca^+ , and Sc^{2+} ions, all with a valence $4s$ electron, as part of our continuing study to understand the importance of the various contributing mechanisms, the series in this case starting with the neutral alkali atom, potassium, and involving the adjacent isoelectronic ions Ca^+ and Sc^{2+} with increasing charges. In the neutral scandium atom, as in general for elements in the $3d$ transition-metal series and the neighboring noble-metal atom

copper, the $3d$ and the $4s$ levels are close in energy. Correspondingly in the case of Sc^{2+} ion, the $3d$ and the $4s$ levels are expected to be also close in energy with either the $3d$ or $4s$ levels occupied. We are concentrating in this work on the Sc^{2+} state with $4s$ as the valence orbital because the series involving this ion and K and Ca^+ involves trends over isoelectronic ions with different charges, which provide a different perspective from the trends in series involving similar charges, as in the case of neutral alkali-metal atoms [3,4] or the singly charged isoelectronic alkaline-earth atoms [4]. It also allows a comparison with the trends in the rather light lithiumlike series [5] with a single core ($1s$) as one goes to increasing charges in the series. The availability of accurate experimental values for K and Ca^+ [6,7] provides a further check on the accuracy of the method used. At the moment no experimental value for the hyperfine field for Sc^{2+} ion is available to our knowledge. We hope the result of our investigation on Sc^{2+} will stimulate an experimental study for this ion, and also that calculations of the hyperfine interaction in these ions might be carried out in the future using different procedures [8–10], since we believe that a comparison with experiment and between the results of different procedures leads to a better understanding of the features of all the procedures.

In Sec. II we present a brief summary of the RLCMBPT procedure. Section III presents the results of our investigation of the magnetic hyperfine fields in K and Sc^{2+} and a discussion and comparison with the results from experiment. The conclusions from our work are listed in Sec. IV.

II. PROCEDURE

The RLCMBPT procedure, and its application both to the hyperfine field problem as well as to other properties of at-

oms, has been described in previous papers [1–5]. We will therefore only give a brief summary of those points relevant to our present work for the sake of completeness. Thus, to predict various physical properties of atomic systems, one needs a complete knowledge of the electronic wave functions of the system. This can be obtained by solving the equation

$$H\Psi_0 = E\Psi_0, \quad (1)$$

where H is the relativistic Hamiltonian of the system, E is the total energy, and Ψ_0 the many-electron wave function of the system involved. The relativistic many-electron Hamiltonian for an atomic system with nuclear charge ζe and N electrons is given by

$$H = \sum_{i=1}^N (c\boldsymbol{\alpha}_i \cdot \mathbf{p}_i + \beta_i mc^2) - \sum_{i=1}^N \frac{\zeta e^2}{r_i} + \sum_{i>j} \frac{e^2}{r_{ij}}, \quad (2)$$

where $\boldsymbol{\alpha}_i$ and β_i are the Dirac matrices for the i th electron, \mathbf{p}_i is its momentum operator, \mathbf{r}_i is its radius vector with respect to the nucleus, and r_{ij} is the distance between the i and j electrons. The Hamiltonian we use does not include the effect of the Breit interaction and other radiative effects, since it has been shown in previous work [1–5] that these interactions are not very important in effect on the hyperfine interaction in the type of systems we would be considering, which have a single s electron orbiting outside a system of closed shells. The exact solution for the wave function Ψ_0 in Eq. (1) for this Hamiltonian is difficult to obtain because of the Coulomb $1/r_{ij}$ interaction between the electrons [11–13]. With the RLCMBPT procedure, a perturbation approach is used to solve this problem by separating H into two parts, namely,

$$H = H_0 + H', \quad (3)$$

where H_0 refers to the zero-order approximation for H , the eigenfunction of which can be solved accurately and $H' = H - H_0$ is a perturbation Hamiltonian.

The zero-order Hamiltonian H_0 is given by

$$H_0 = \sum_{i=1}^N (c\boldsymbol{\alpha}_i \cdot \mathbf{p}_i + \beta_i mc^2) - \sum_i \frac{\zeta e^2}{r_i} + \sum_i V(r_i) \quad (4)$$

in which $V(r_i)$ is a one-electron potential, for which the eigenfunction Φ_0 is given by

$$H_0\Phi_0 = E_0\Phi_0, \quad (5)$$

and can be solved precisely. As explained in earlier literature [1,14], it has been the usual practice to choose for $V(r_i)$, a V^{N-1} potential defined by the relation

$$\langle a|V^{N-1}|b\rangle = \sum_{n=1}^{N-1} \left[\left\langle an \left| \frac{e^2}{r_{12}} \right| bn \right\rangle - \left\langle an \left| \frac{e^2}{r_{12}} \right| nb \right\rangle \right] \quad (6)$$

with n representing occupied states of the atom. The perturbation Hamiltonian H' defined in Eq. (3) is then written as

$$H' = H - H_0 = \sum_{i>j} \frac{e^2}{r_{ij}} - \sum_i V_i^{N-1}. \quad (7)$$

The exact eigenfunction Ψ_0 of the many-particle Hamiltonian H can now be expressed by the linked-cluster expansion [1,15,16] in terms of the eigenfunction Φ_0 (energy eigenvalue E_0) of H_0 , namely,

$$\Psi_0 = \sum_n^L \left[\frac{H'}{E_0 - H_0} \right]^n \Phi_0. \quad (8)$$

Once Ψ_0 is determined, the hyperfine properties of the atomic system can then be calculated as the expectation value of the hyperfine interaction Hamiltonian H'_{hyp} over Ψ_0 .

For a relativistic treatment of the magnetic hyperfine interaction, the electron-nuclear hyperfine interaction Hamiltonian is given by [1,13]

$$H'_{\text{hyp}} = \sum_i ec\boldsymbol{\alpha}_i \cdot \frac{\boldsymbol{\mu}_i \times \mathbf{r}_i}{r_i^3}, \quad (9)$$

where $\boldsymbol{\mu}_i$ is the magnetic moment of the nucleus. In terms of H'_{hyp} , the theoretical expression for the experimentally measured hyperfine constant in the spin-Hamiltonian term $\mathbf{AI} \cdot \mathbf{J}$ is given by [1]

$$A_J = \frac{1}{IJ} \langle \Psi_0 | H'_{\text{hyp}} | \Psi_0 \rangle = \sum_{m,n}^L \left\langle \Phi_0 \left[\frac{H'}{E_0 - H_0} \right]^m H'_{\text{hyp}} \left[\frac{H'}{E_0 - H_0} \right]^n \Phi_0 \right\rangle. \quad (10)$$

The vectors \mathbf{I} and \mathbf{J} refer to the nuclear spin and total angular momentum, respectively. The quantities I and J characterize the eigenvalues $I(I+1)$ and $J(J+1)$ of \mathbf{I}^2 and \mathbf{J}^2 . The various terms in Eq. (10) corresponding to different m and n values are referred to as (m,n) -order terms. The value $(m+n)$ for each term represents the order of the perturbation in H' , each (m,n) term being expressible as a diagram representing a specific mechanism, through the use of rules given in earlier work [1,2]. The zeroth-order perturbation term $(0,0)$ is referred to as direct or valence contribution to the hyperfine constant. The first-order contributions $(1,0)$ or $(0,1)$ terms represent the ECP effect, and the second-order perturbation $(1,1)$ and $(2,0)$ or $(0,2)$ terms represent the many-body correlation effect.

The major diagrams evaluated in this work are given in Figs. 1–5. Figure 1 is the diagrammatic representation of the zero-order (valence or direct contribution) Hartree-Fock result, only the unpaired valence electron contributing to the direct effect. The ECP effect is represented by Fig. 2(a), and Fig. 2(b) represents a phase-space diagram associated with the ECP effect. This phase-space effect arises because the valence s shell is only half filled and it is therefore possible for a core electron with spin antiparallel to the valence elec-

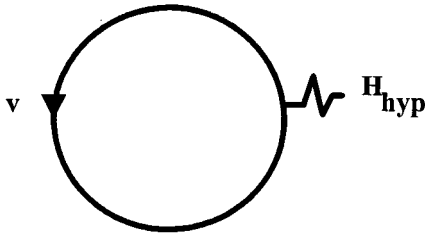


FIG. 1. Diagrammatic representation of the zero-order (0,0), valence contribution to the hyperfine field.

tron to be excited into the available empty state in the valence s shell. The effects of such an excitation cannot be canceled out between antiparallel spin core electrons because a similar excitation into the already occupied state with spin parallel to the valence state cannot occur. Figures 3(a) and 3(b) are typical exclusion principle violation (EPV) diagrams [1,4] and Figs. 3(c) and 3(d) are consistency diagrams [1]. Figures 4(a) and 4(b) show the (0,2) correlation diagrams while Figs. 5(a) and 5(b) show the (1,1) correlation diagrams. The diagrams in Figs. 4 and 5 represent the contribution to the hyperfine interaction from simultaneous excitations of two electrons due to the Coulomb interaction between them, representing true many-body effects. The diagrams in Fig. 3 are essentially one-electron diagrams, which correct for the use of a restricted Hartree-Fock potential in H_0 . The rules for the mathematical expressions represented by these diagrams, which one needs to evaluate to obtain their contributions to the hyperfine constant, have been given in the literature [1,2]. The contributions from perturbation terms higher than second order to the hyperfine interaction are in general found to be quite small in most atoms studied so far [1–4].

Often the experimental results for hyperfine interactions in atoms are quoted in terms of hyperfine fields H_{hyp} at the nuclei, the latter being the more pertinent quantities to consider in discussing the trends between different atomic systems since they are purely electronic in origin and do not involve nuclear magnetic moments. The relationship between H_{hyp} and the hyperfine constant A is given by [4]

$$H_{\text{hyp}} = \left[\frac{2\pi}{\gamma_I} \right] AJ, \quad (11)$$

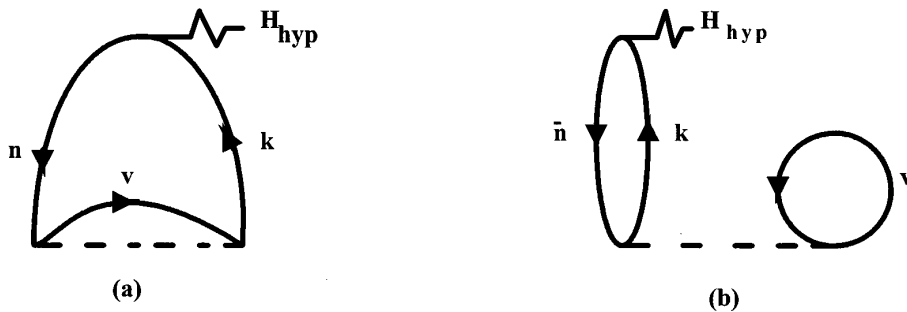


FIG. 2. Diagrams representing the (a) ECP, (b) phase-space contributions to the hyperfine field.

where $\gamma_I = \mu_I / I\hbar$ is the magnetogyric ratio of the nucleus involved, μ_I is the nuclear moment, and J is the net electronic angular momentum. Using the relation $g_I = \gamma_I \hbar / \mu_N = (1/I)(\mu_I / \mu_N)$, μ_N being the nuclear magneton, it is convenient to express H_{hyp} in the form

$$H_{\text{hyp}} = \left[\frac{\pi \hbar}{\mu_N} \right] \left[\frac{A}{g_I} \right] = (6.559355) \left[\frac{A}{g_I} \right] \times 10^{-2} \text{ T}. \quad (12)$$

The numerical constant in Eq. (12) was obtained using $\mu_N = 5.050786 \times 10^{-27} \text{ J/T}$, $\hbar = 1.05457266 \times 10^{-34} \text{ J sec}$ [17], and A in units of MHz.

III. RESULTS AND DISCUSSIONS

The calculated contributions to the hyperfine field arising from the main mechanisms, namely, valence ECP and correlation effects, as well as the net hyperfine fields for the systems of interest in the present work are listed in Tables I and II for the isoelectronic K, Ca^+ , and Sc^{2+} systems (all with a single $4s$ valence electron) and Na, K, and Rb systems (with valence electron in $3s$, $4s$, and $5s$ states), respectively. Also presented in these tables are the corresponding total hyperfine fields from experimental measurement. Table III shows a more detailed summary of the calculated contributions from individual mechanisms, which are grouped together under ECP and correlation in Table I for K, Ca^+ , and Sc^{2+} . Considering Table I first, the second column in Table I gives the valence electron contribution, which is the leading contributor in relativistic theory. These contributions explain only a part, although a major one, of the experimental results amounting to about 66% of the experimental value [6] in K and about 76% of the experimental value [7] in Ca^+ . There was therefore the need to go beyond the basic restricted Hartree-Fock procedure.

The results in the third column of Table I come from the first-order (0,1) diagrams in Figs. 2 and 3. The ECP, EPV, consistency, and phase-space contributions are grouped together (and referred to as ECP in Table I) because they represent one-electron effects beyond zeroth-order valence contributions. As a group, they give the net contribution arising from the polarization of the core orbitals. It was assumed, when the basis sets are generated, that all electrons with the real quantum numbers n and j possessed identical radial wave functions. This means that the core states cannot contribute to the hyperfine interactions in the zeroth-order ap-

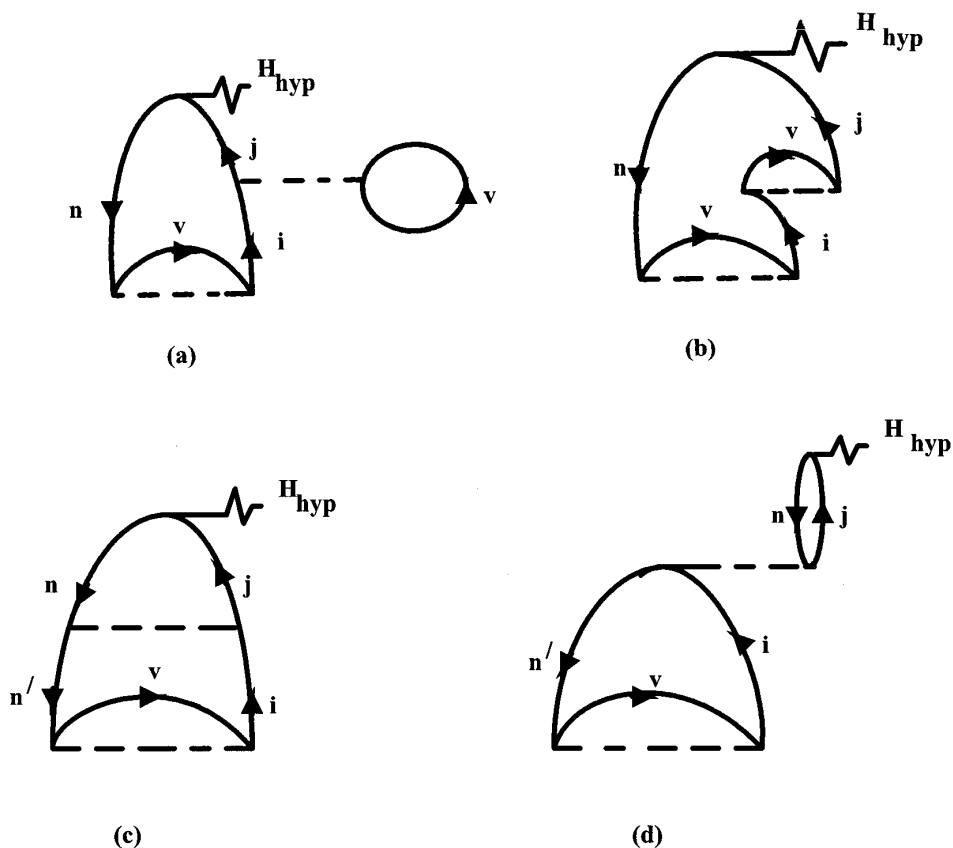


FIG. 3. Diagrams representing (a) EPV (direct), (b) EPV (exchange), (c) and (d) (0,2) types of consistency effects. The index v refers to the occupied valence s state, the indices n, n' represent core states, and i, j represent excited states.

proximation because the contributions of those electrons in a given shell with opposing spins cancel one another exactly. This assumption is not correct, since not all the electrons in a given core shell will experience exchange interactions with the single valence electron, the core electrons with spin parallel to that of the valence electron being the ones that are subject to the exchange interactions while the antiparallel spin core states are not. Consequently, the parallel and antiparallel spin core states in each shell will have different radial wave functions. The result is that the core electrons can make a nonvanishing contribution to the hyperfine field. The ECP diagrams [Fig. 2(a)] [4] represent a first-order correction due to this effect. The other diagrams [Figs. 2(b) and 3], grouped under the umbrella of net ECP contributions, represent additional first- and second-order contributions, which

are less important than the diagram in Fig. 2(a) and make fewer contributions but are all associated with different interactions [2,4] between the valence electron and core electrons with spins parallel and antiparallel to the valence spin.

The fifth column of Table I represents the net contributions from the (0,2) correlation diagram in Fig. 4 and the (1,1) correlation diagram in Fig. 5. These diagrams all involve two simultaneously excited electrons and this leads to true many-body contributions to the field. Our total calculated hyperfine fields are listed in the seventh column of Table I and are seen to be in excellent agreement with experimental results, differing by only about 2% in the case of K and about 3% in the case of Ca^+ . This is essentially in complete agreement when we take into account experimental and computational errors.

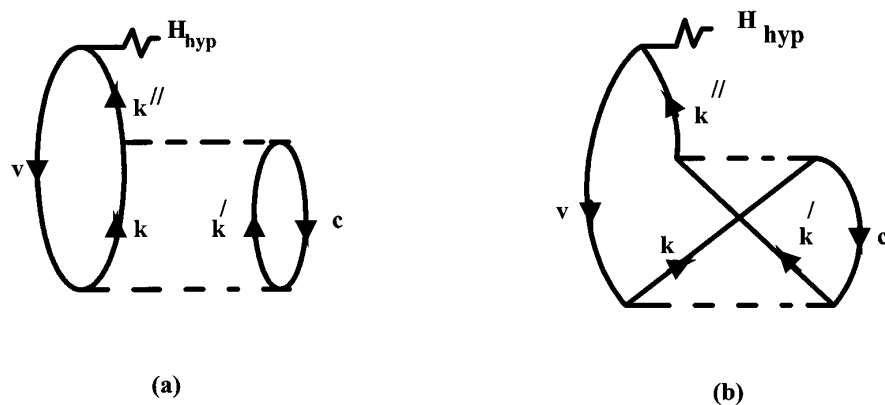


FIG. 4. Typical second-order (0,2) correlation diagrams. They represent (a) direct and (b) exchange correlation contributions to the hyperfine field.

TABLE I. Contributions from direct, ECP, and correlation mechanisms to the hyperfine fields (Tesla) in the isoelectronic systems K, Ca^+ , and Sc^{2+} with $4s$ valence electron.

System	H_{val}	H_{ECP}	$H_{\text{ECP}}/H_{\text{val}}$	H_{corr}	$H_{\text{corr}}/H_{\text{val}}$	H_{total}	H_{Expt}
K	37.60	7.03	0.19	12.18	0.32	56.81	58.02 ^a
Ca^+	103.40	17.20	0.17	15.30	0.15	135.30 ^b	140.3 ^c
Sc^{2+}	191.19	26.23	0.14	21.87	0.11	239.29	

^aSee Ref. [6].

^bSee Ref. [4].

^cSee Ref. [7].

We will now consider the trends in the ECP and correlation contributions to the hyperfine fields in both the alkali series (Na,K,Rb) and the alkalilike series (K, Ca^+ , Sc^{2+}) and compare the two. The ratio $H_{\text{ECP}}/H_{\text{val}}$ and $H_{\text{corr}}/H_{\text{val}}$ for both series can be found in columns 4 and 6, respectively in Tables I and II. Unfortunately, the individual contributions to the hyperfine field (direct, ECP, and correlation) cannot be measured. However, there is strong indirect support for the accuracy of the theoretical values for them in view of the very good agreement between the calculated [4] and experimental values [6,7,18,19] of the total fields. Hence one could consider the trends in $H_{\text{ECP}}/H_{\text{val}}$ and $H_{\text{corr}}/H_{\text{val}}$ as also being quite accurate. It has been the practice in considering trends to examine the latter ratios, rather than the absolute values of H_{ECP} and H_{corr} . The main reason for this is that since H_{val} is the largest contributor and varies substantially in going from one system to another, it is more convenient to look at the ‘normalized’ ratio, which is now a dimensionless fraction. Additionally, since one could expect the behavior of the hyperfine vertices in the ECP and major correlation diagrams to vary in a reasonably similar manner as the hyperfine vertex involving only the valence state as in the diagram in Fig. 1 for the zero-order valence contribution, the ratio would be expected to be primarily representative of the influence of electron-electron interactions of the one-electron and multi-electron types for the ECP and correlation effects.

In the alkalilike series (K, Ca^+ , Sc^{2+}), the ratio $H_{\text{ECP}}/H_{\text{val}}$ decreases continuously in going from K to Sc^{2+} . The decrease in $H_{\text{ECP}}/H_{\text{val}}$ from K to Ca^+ is more rapid than from Ca^+ to Sc^{2+} . For the alkali series on the other hand, the decrease of this ratio as one goes from Na to Rb is slower, the values for K and Rb being nearly the same. The trend of

a decrease of this ratio in both series (Na, K, and Rb) and (K, Ca^+ , Sc^{2+}) can be understood using the fact that both systems are rather similar. Each atom in the series has a single s valence electron and p outermost cores. The rapid decrease of the ratio from K to Ca^+ through to Sc^{2+} is expected to be due to the tighter binding of the core shell electrons in the ions as compared to the neutral atom K. This makes the core electrons less deformable than those for the neutral alkali atoms under the influence of the exchange perturbation potential due to the valence electrons. For the series Na to Rb, where the number of cores steadily increases, there is also a tightening of the core electrons because they experience a more attractive potential as the nuclear charge increases due to more incomplete shielding of the core electrons by each other, and the valence electron, as one adds extra nuclear charges and electrons. This effect is, however, not expected to be as pronounced as when one removes an entire electron from a neighboring atom in the period, for instance, in going from K to Ca^+ and Ca^+ to Sc^{2+} , leading to the more rapid decrease for $H_{\text{ECP}}/H_{\text{val}}$ over this series than over the alkali-atom series Na, K, and Rb.

The ratio of correlation contribution to direct is shown in column 6 in Table I for K, Ca^+ , and Sc^{2+} systems and in Table II also in column 6 for Na, K, and Rb. There is an interesting difference in trend between the two series. For the alkalilike series, K, Ca^+ , and Sc^{2+} the ratio $H_{\text{corr}}/H_{\text{val}}$ decreases steadily in going from K to Sc^{2+} ranging from 0.32 for K to 0.11 for Sc^{2+} . There is also a sharp drop in $H_{\text{corr}}/H_{\text{val}}$ from K to Ca^+ , while there is a slower decrease from Ca^+ to Sc^{2+} . For the alkali series (Na,K,Rb), on the other hand, the ratio increases as we move down the series from Na to Rb. This trend is opposite to the trend observed

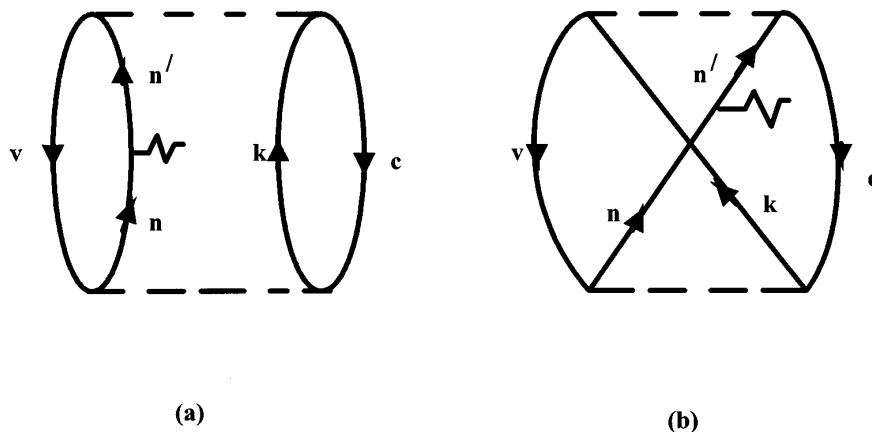


FIG. 5. Second-order (1,1)-type correlation diagrams. (a) and (b) are the direct and exchange types of diagrams, respectively.

TABLE II. Contributions from direct, ECP, and correlation mechanisms to the hyperfine fields (tesla) in the alkali-metal atoms Na, K, and Rb.

Atoms	H_{val}	H_{ECP}	$H_{\text{ECP}}/H_{\text{val}}$	H_{corr}	$H_{\text{corr}}/H_{\text{val}}$	H_{total}	H_{Expt}
Na	27.9	6.10	0.22	4.2	0.15	38.50 ^a	39.30 ^b
K	37.6	7.03	0.19	12.18	0.32	56.81	58.02 ^c
Rb	80.7	16.10	0.20	26.6	0.33	123.2 ^a	122.2 ^d

^aSee Ref. [4].

^bSee Refs. [18], [19].

^cSee Ref. [6].

^dSee Ref. [19].

in the $H_{\text{ECP}}/H_{\text{val}}$ ratio where there is a continuous decline in going from Na to Rb. Also, it is opposite to that found for $H_{\text{corr}}/H_{\text{val}}$ in the alkalilike series. There is a sharp increase in the ratio $H_{\text{corr}}/H_{\text{val}}$ from Na (0.15) to K (0.32) but a somewhat more gradual increase from K (0.32) to Rb (0.33).

In attempting to understand the physical reasons for the trends just described in $H_{\text{corr}}/H_{\text{val}}$, we shall first consider the alkali series. The observed increase in $H_{\text{corr}}/H_{\text{val}}$ can be explained by noting that the major correlation diagram in Fig. 4 can be viewed as representing a van der Waals type of interaction between the outermost core electron and valence electron involving their mutual polarization by the Coulomb interaction between them. This van der Waals type of effect is expected to depend on two factors. These are the deformabilities of the core and valence electrons and the average distances between these electrons. The two factors can be seen to compete with each other since increased separation causes a decrease in the correlation effect while an increase in the deformabilities leads to an increase in the correlation effect. An increase in the $H_{\text{corr}}/H_{\text{val}}$ ratio in the alkali series in going from Na to Rb suggests that the deformabilities constitute the dominant factor over separation as we go down

the series, this factor being relatively more dominant between Na and K than between K and Rb. The greater deformability of the valence electron is a result of the fact that it tends to get more loosely bound as a consequence of the tighter binding of the core electrons in going to larger alkali atoms and the consequent greater screening of the nuclear charge by them, making the valence electron experience a weaker attractive potential. The more loosely bound valence electron also leads to a larger separation between the core and valence electrons but, as just remarked, it appears that the opposing effect of this factor in going from Na to K to Rb seems to be more than counterbalanced by the increasing deformability of the valence electrons. The opposite trend observed for the alkalilike systems K, Ca^+ , and Sc^{2+} for $H_{\text{corr}}/H_{\text{val}}$ as compared to that for the alkali-atom series Na, K, and Rb is expected physically because in going to positive ions from an isoelectronic neutral atom, both the core and valence electrons get more tightly bound and therefore less deformable with respect to the perturbation due to the correlation effect. It is intriguing to try to explain physically the lower decrease from Ca^+ to Sc^{2+} for $H_{\text{corr}}/H_{\text{val}}$ as compared to that from K to Ca^+ . It could partly be due to the influence of a possible increase in the core-valence separation due to greater contraction of the core electron shells as compared to valence.

IV. CONCLUSION

The net results obtained in the present work for the hyperfine fields in K and Ca^+ by the RLCMBPT procedure are found to be in excellent agreement with experimental results for these systems. There are no experimental data for Sc^{2+} system currently available and therefore no comparison with theory is possible. It is interesting to note just as for the alkali series, there are interesting trends in the ECP and correlation contributions to the total hyperfine fields in the alkalilike series (K, Ca^+ , Sc^{2+}). The trends produced in both these series can be analyzed in terms of the features of the core and valence electron distributions. The factors influencing the behavior of ECP and correlation effects within each of these series are the deformabilities of the valence shell, the effective nuclear charges of the system, and the average distance between core and valence electrons. We hope that the present work will encourage experimental determination of the hyperfine field in the Sc^{2+} to allow comparison with our theoretical results. We also hope that other investigators will make similar calculations using other methods for the alkalilike systems so as to allow a comparison of the results with those of the relativistic many-body perturbation theory technique used here.

TABLE III. Detailed list of contributions from different mechanisms to the hyperfine field (tesla) in K, Ca^+ , and Sc^{2+} .

Mechanism	K	Ca^+	Sc^{2+}
Valence	37.6	103.4	191.19
ECP	6.6	17.2	27.01
Phase space	1.03	1.6	1.67
EPV	-0.7	-1.9	-2.9
Consistency	0.1	0.3	0.45
Net ECP	7.03	17.2	26.23
(0,2) correlation	11.49	14.7	20.97
(1,1) correlation	-0.11	-0.4	-0.60
Total second-order correlation	11.38	14.3	20.37
Third order	0.8	1.0	1.5
Total	56.81	135.9	239.29
Experimental	58.02 ^a	139.99 ^b	
		140.30 ^c	
		142.39 ^d	

^aSee Ref. [6].

^bSee Ref. [7(a)].

^cSee Ref. [7(b)].

^dSee Ref. [7(c)].

- [1] T. P. Das, *Hyperfine Interact.* **34**, 189 (1987).
- [2] N. C. Dutta, C. Matsubara, R. T. Pu, and T. P. Das, *Phys. Rev. Lett.* **21**, 1139 (1968); S. N. Panigrahy, R. W. Dougherty, S. Ahmad, K. C. Mishra, J. Andriessen, and T. P. Das, *Phys. Rev. A* **43**, 2215 (1991), and references therein.
- [3] E. S. Chang, R. T. Pu, and T. P. Das, *Phys. Rev.* **174**, 1 (1968); M. Vajed-Samii, J. Andriessen, B. P. Das, S. N. Ray, T. Lee, and T. P. Das, *J. Phys. B* **15**, L379 (1982); *Phys. Rev. Lett.* **48**, 1330 (1982), and references therein.
- [4] X. Yuan, S. N. Panigrahy, R. W. Dougherty, J. Andriessen, and T. P. Das, *Phys. Rev. A* **52**, 197 (1995), and references therein.
- [5] S. N. Panigrahy, R. W. Dougherty, J. Andriessen, and T. P. Das, *Phys. Rev. A* **44**, 121 (1991).
- [6] A. Beckmann, K. D. Boklen, and D. Elke, *Z. Phys.* **270**, 173 (1974).
- [7] (a) A. T. Goble and S. Maleki, *Phys. Rev. A* **42**, 649 (1990); (b) E. Silverans, L. Vermeeren, R. Neugart, P. Lieven, and the ISOLDE Collaboration, *Z. Phys. D* **18**, 351 (1991); (c) F.M. Kelly, H. Kuhn, and A. Pery, *Proc. Phys. Soc. London Sec. A* **67**, 450 (1954).
- [8] J. L. Heully and A. M. Martensson-Pendrill, *Phys. Scr.* **31**, 169 (1985); S. Garpman, I. Lindgren, and J. Morrison, *Z. Phys. A* **276**, 167 (1976).
- [9] V. A. Dzuba, V. V. Flambaum, and O. P. Sushkov, *J. Phys. B* **17**, 1953 (1984).
- [10] J. Andriessen, H. Postma, A. M. Van den Brink, and T. P. Das, *Phys. Rev. A* **45**, 1389 (1992).
- [11] H. A. Bethe and E. E. Salpeter, *Quantum Mechanics of One- and Two-Electron Atoms* (Academic, New York, 1959).
- [12] I. P. Grant, *Proc. Roy. Soc. London Ser. A* **262**, 555 (1961); M. A. Coulthard, *Proc. Phys. Soc.* **91**, 44 (1961); J. P. Desclaux, D. F. Mayers, and F. O'Brien, *J. Phys. B* **4**, 631 (1971).
- [13] T. P. Das, *Relativistic Quantum Mechanics of Electrons* (Harper and Row, New York, 1973).
- [14] H. P. Kelly, *Phys. Rev.* **136**, B896 (1964); H. P. Kelly, *ibid.* **131**, 684 (1963).
- [15] K. A. Brueckner, *Phys. Rev.* **100**, 36 (1956).
- [16] J. Goldstone, *Proc. R. Soc. London Ser. A* **239**, 267 (1957).
- [17] Pramila Raghavan, *Atomic Data and Nuclear Data Tables*, Vol. 42 (Academic Press, New York, 1989); E. R. Cohen and B. N. Taylor, *Rev. Mod. Phys.* **59**, 1121 (1987).
- [18] K. H. Liao, R. Gupta, and W. Happer, *Rev. Mod. Phys.* **8**, 2792 (1973).
- [19] E. Arimondo, M. Inguscio, and P. Violino, *Rev. Mod. Phys.* **49**, 31 (1977).